PNAS RESEARCH ARTICLE | NEUROSCIENCE

Histone methylation-mediated microRNA-32-5p down-regulation in sensory neurons regulates pain behaviors via targeting Cav3.2 channels

Renfei Qi[a,b,1], Junping Cao[a,b,c,1], Yufang Sun[a,b,d,1], Yanping Li[a,b], Zitong Huang[a,b], Dongsheng Jiang[e], Xing-Hong Jiang[a,b], Terrance P. Snutch[f,g], Yuan Zhang[h,i,2], and Jin Tao[a,b,d,2]

Edited by Hee-Sup Shin, Institute for Basic Science, Daejeon, South Korea; received September 23, 2021; accepted January 13, 2022

microRNA (miRNA)–mediated gene regulation has been studied as a therapeutic approach, but its functional regulatory mechanism in neuropathic pain is not well understood. Here, we identify that miRNA-32-5p (miR-32-5p) is a functional RNA in regulating trigeminal-mediated neuropathic pain. High-throughput sequencing and qPCR analysis showed that miR-32-5p was the most down-regulated miRNA in the injured trigeminal ganglion (TG) of rats. Intra-TG injection of miR-32-5p agomir or overexpression of miR-32-5p by lentiviral delivery in neurons of the injured TG attenuated established trigeminal neuropathic pain. miR-32-5p overexpression did not affect acute physiological pain, while miR-32-5p down-regulation in intact rats was sufficient to cause pain-related behaviors. Nerve injury increased the methylated histone occupancy of binding sites for the transcription factor glucocorticoid receptor in the miR-32-5p promoter region. Inhibition of the enzymes that catalyze H3K9me2 and H3K27me3 restored the expression of miR-32-5p and markedly attenuated pain behaviors. Further, miR-32-5p–targeted Cav3.2 T-type Ca^{2+} channels and decreased miR-32-5p associated with neuropathic pain caused an increase in Cav3.2 protein expression and T-type channel currents. Conversely, miR-32-5p overexpression in injured TG suppressed the increased expression of Cav3.2 and reversed mechanical allodynia. Together, we conclude that histone methylation-mediated miR-32-5p down-regulation in TG neurons regulates trigeminal neuropathic pain by targeting Cav3.2 channels.

Cav3.2 | T-type Ca^{2+} channels | microRNA | neuropathic pain | trigeminal ganglion neurons

Significance

In this study, we identify microRNA-32-5p (miR-32-5p) as a key functional noncoding RNA in trigeminal-mediated neuropathic pain. We report that injury-induced histone methylation attenuates the binding of glucocorticoid receptor to the promoter region of the *miR-32-5p* gene and decreases the expression of miR-32-5p, in turn promoting the development of neuropathic pain through regulation of Cav3.2 channels. miRNA-mediated gene regulation has been proposed as a therapeutic approach in neuropathic pain. Our findings identify miR-32-5p replenishment as a therapeutic strategy for treating chronic neuropathic pain.

Chronic neuropathic pain is often associated with injuries or pathological defects of the somatosensory system, which is often observed in patients with traumatic nerve injury, diabetes, or cancers (1, 2). The current widely used therapeutic strategies with opioids and nonsteroidal anti-inflammatory drugs are far from satisfactory, due to limited effectiveness and adverse effect of addiction (2). Thus, identifying the mechanisms underlying neuropathic pain is essential for the development of innovative treatments for this disorder. Trigeminal ganglion (TG) neurons are primary sensory neurons that detect a variety of noxious and innocuous stimuli and convey peripheral signals to the central nervous system and are an important analgesic target (3). Accumulating evidence suggests that injuries of peripheral nerve can result in remarkable changes of expression pain-associated genes in the TG at both messenger RNA (mRNA) and protein levels (4) and subsequently lead to the initiation and persistence of neuropathic pain (5). Therefore, a deep understanding of transcriptomic changes of pain-associated genes in the TG after peripheral nerve injury will pave the way for the development of novel therapeutic options for neuropathic pain.

microRNAs (miRNAs) are small single-stranded noncoding RNAs (typically containing about 22 nucleotides) that regulate gene expression by binding to 3′-untranslated regions (3′-UTRs) of target mRNAs and blocking their translation (6). Studies have implicated miRNA-mediated regulation in a number of diseases, including cancer, resulting in this regulation being studied as a therapeutic strategy (7) and with several preclinical and clinical trials of miRNA-based therapeutics having been initiated (8). In the mammalian nervous system, emerging evidence has identified certain miRNAs as being implicated as potential pain modulators (9). For instance, in TG neurons, miRNA expression is differentially modulated following inflammatory muscle pain (10). miRNA-32-5p (miR-32-5p) is abundant and highly conserved across species and shown to modulate various processes, such as adipose metabolism (11), and diseases, such as cancer (12) and myocardial fibrosis (13). Moreover, down-regulation of miR-32-5p expression induced by high glucose inhibits cell-cycle progression via PTEN up-regulation in bone marrow-derived mesenchymal stem cells (14). miR-32-5p

Author contributions: J.T. designed research; R.Q., J.C., Y.S., Y.L., Z.H., and Y.Z. performed research; R.Q., J.C., Y.S., Y.L., Z.H., X.-H.J., Y.Z., and J.T. analyzed data; and J.C., D.J., T.P.S., and J.T. wrote the paper.

The authors declare no competing interest.

This article is a PNAS Direct Submission.

[1]R.Q., J.C., and Y.S. contributed equally to this work.

[2]To whom correspondence may be addressed. Email: taoj@suda.edu.cn or yuanzhang@suda.edu.cn.

This article contains supporting information online at http://www.pnas.org/lookup/suppl/doi:10.1073/pnas.2117209119/-/DCSupplemental.

Published March 30, 2022.

has also been shown to promote lipid metabolism in oligodendrocytes and to increase myelin production (15). Although limited evidence suggests a potential modulatory function of miR-32-5p in nervous system disorders, it remains unclear whether and how TG neuronal miR-32-5p participates in nociceptive responses.

In the present study, we identified miR-32-5p in rat TG neurons as an important miRNA concerning nociception. Histone methylation attenuated the binding of glucocorticoid receptor (GR) to the promoter of the *miR-32-5p* gene and decreased the expression of miR-32-5p after nerve injury. We also demonstrate that miR-32-5p expression levels underlie the maintenance of neuropathic pain through the regulation of Cav3.2 T-type calcium (Ca^{2+}) channels, a low voltage-activated channel that regulates subthreshold excitability in sensory neurons and contributes to low-threshold exocytosis related to pain symptoms (16). Our results highlight the pivotal role of miR-32-5p in Cav3.2 channel regulation in contributing to trigeminal-mediated neuropathic pain. This mechanistic understanding may pave the way for the development of novel therapeutic strategies for chronic neuropathic pain treatment.

Results

miR-32-5p Is Down-Regulated in TG Neurons after Chronic Constriction Injury of the Infraorbital Nerve. Trigeminal neuropathic pain was induced by unilateral chronic constriction injury of the infraorbital nerve (CCI-ION) in rats. Compared with sham-operated rats, rats subjected to CCI-ION displayed a dramatic decrease in the mechanical pain threshold on days 14, 21, and 28 post–CCI-ION (Fig. 1*A*). To search for novel miRNAs and regulatory networks that are critical for the pathogenesis of neuropathic pain, we performed a genome-wide gene-expression profile analysis of TGs on day 14 after CCI-ION. Among the 18 TG-rich miRNAs showing significant expression decrease (Fig. 1*B*), 12 were confirmed by qPCR analysis as showing more than 50% down-regulation in the ipsilateral TG tissue of CCI-ION rats (Fig. 1*C*). Among them, miR-32-5p was the most robustly down-regulated (Fig. 1*C*). Therefore, we chose to analyze the expression and function of miR-32-5p. By using strand-specific primers for reverse transcription, we found that the miR-32-5p transcript was abundant in rat TGs (Fig. 1*D* and *SI Appendix*, Fig. S1). qPCR analysis showed that the expression level of miR-32-5p was higher (~3.1-fold) in rat TGs compared to that in brain (Fig. 1*E*). Furthermore, we investigated the time course of *miR-32-5p* expression in ipsilateral TG tissue after CCI-ION or sham operation by qPCR. The miR-32-5p level was significantly decreased on day 14 and maintained on day 28 in CCI-ION rats (Fig. 1*F*). The mRNA level did not significantly differ in sham-operated rats at any of the tested time points (Fig. 1*F*). We further determined the cellular localization of miR-32-5p in the TG. In situ hybridization revealed that miR-32-5p was strongly expressed in small- and medium-sized neurons (Fig. 1*G*). In injured TGs on day 14 after CCI-ION, miR-32-5p expression was decreased (Fig. 1*G*). Fluorescence in situ hybridization (FISH) combined with immunostaining showed that miR-32-5p was primarily colocalized with the neuronal marker NeuN and rarely/not colocalized with the satellite glial marker glutamine synthetase (GS) (Fig. 1*H*).

miR-32-5p Regulates Nociceptive Behaviors. To assess the direct contribution of miR-32-5p to neuropathic pain, we unilaterally injected an miR-32-5p mimic (agomir-32-5p) or negative control (agomir-NC) into rat TGs. Administration of agomir-32-5p dramatically attenuated mechanical hyperalgesia in the rats on day 14 post–CCI-ION, while agomir-NC treatment elicited no such effect (Fig. 2*A*). To obtain complementary support for this result, we induced miR-32-5p expression specifically in TG

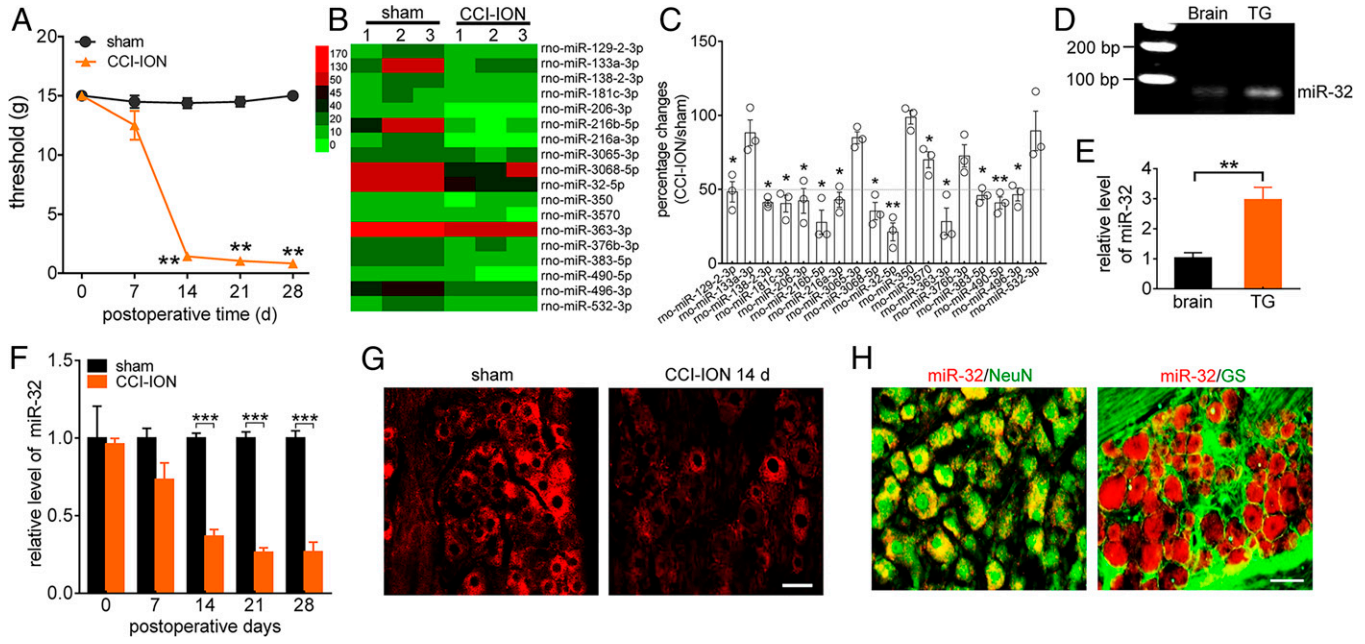

Fig. 1. miR-32-5p is down-regulated in TG neurons after CCI-ION. (*A*) Orofacial response threshold (threshold) to mechanical stimuli in the sham-operated and CCI-ION–operated groups (n = 10 rats per group). $^{**}P < 0.01$ (vs. sham, two-way ANOVA). (*B*) Heat map indicating TG-rich miRNAs showing significant expression decrease in injured TGs. (*C*) qPCR analysis indicating that 12 miRNAs are down-regulated by >50% in ipsilateral TG tissue on day 14 post–CCI-ION. $^{*}P < 0.05$; $^{**}P < 0.01$ (in CCI-ION vs. sham, unpaired t test). (*D*) RT-PCR analysis of miR-32-5p (miR-32) in the brains and TGs of intact rats. The blots shown are representative of three independent experiments. (*E*) qPCR of miR-32-5p expression in rat brain and TGs (n = 5 rats per group). $^{**}P < 0.01$ (vs. brain, unpaired t test). (*F*) The time course of miR-32-5p expression in the ipsilateral TGs in sham and CCI-ION–operated rats (n = 5 to 7 rats per group). $^{***}P < 0.001$ (vs. sham, one-way ANOVA). (*G*) Representative images of miR-32-5p expression in ipsilateral TG tissue on day 14 after CCI-ION or sham operation. (Scale bar, 50 μm.) (*H*) In situ hybridization of miR-32-5p and immunostaining with NeuN or GS. (Scale bar, 50 μm.).

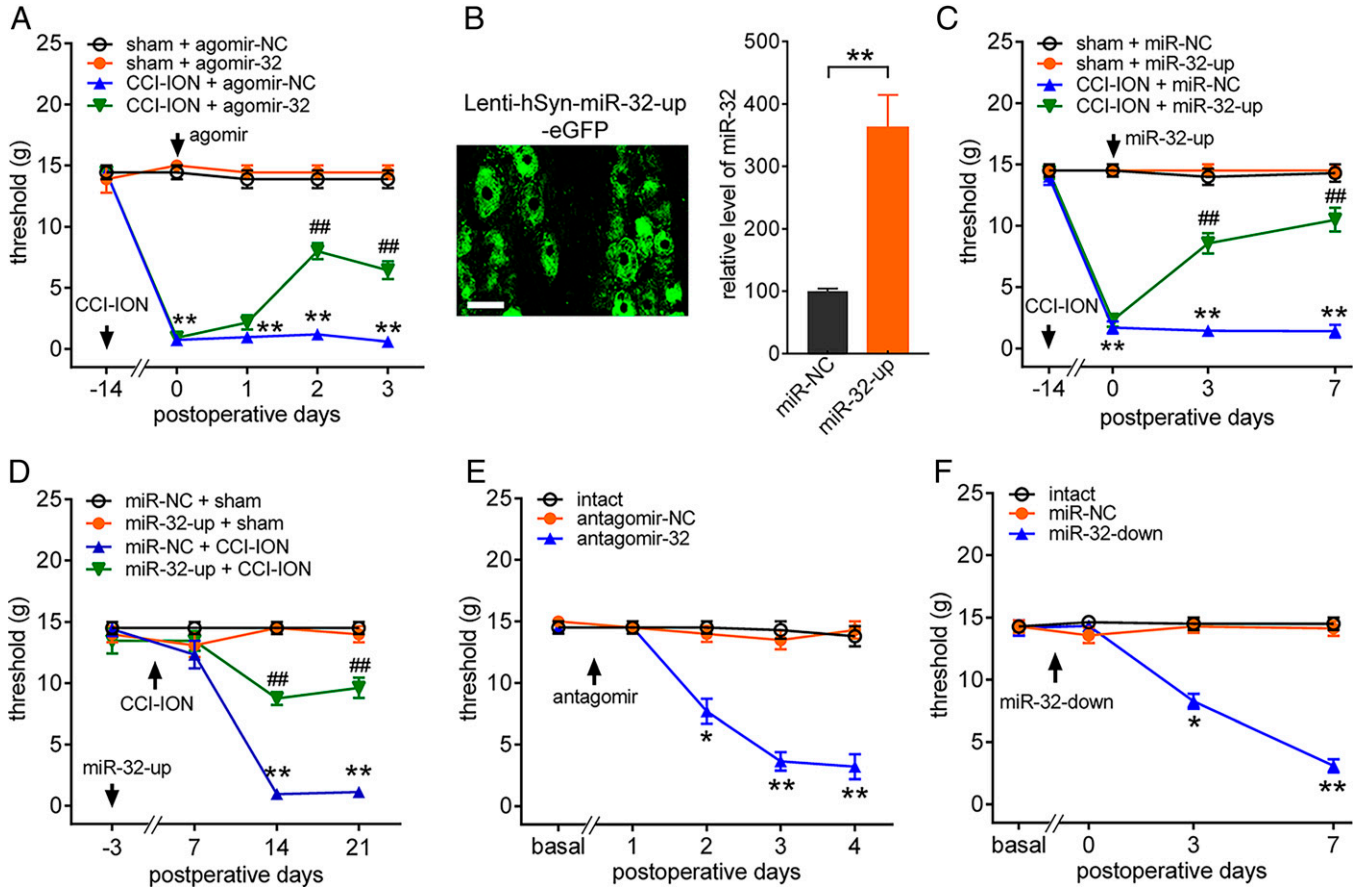

Fig. 2. miR-32-5p regulates pain behavior. (*A*) Intra-TG injection of mir-32-5p (agomir-32)-attenuated mechanical allodynia on day 14 post–CCI-ION (n = 8 to 10 rats per group). $^{**}P < 0.01$ (vs. sham + agomir-NC); $^{\#\#}P < 0.01$ (vs. CCI-ION + agomir-NC) (two-way ANOVA). (*B*, *Left*) Representative image of EGFP immunofluorescence in an intact TG 3 d after injection of a miR-32-up. (Scale bar, 50 μm.) (*B*, *Right*) Summary data showing the increased expression of miR-32-5p in intact TGs on day 3 after intra-TG injection of miR-32-up (n = 6 to 8 rats per group). $^{**}P < 0.01$ (vs. miR-NC, unpaired t test). Data are representative of three independent experiments. (*C*) Intra-TG injection of miR-32-up attenuated mechanical allodynia on day 14 post–CCI-ION (n = 7 to 10 rats per group). $^{**}P < 0.01$ (vs. sham + miR-NC); $^{\#\#}P < 0.01$ (vs. CCI-ION + miR-NC) (two-way ANOVA). (*D*) Preliminary intra-TG injection of miR-32-up prevented the decrease in mechanical threshold induced by CCI-ION (n = 9 or 10 rats per group). $^{**}P < 0.01$ (vs. miR-NC + sham); $^{\#\#}P < 0.01$ (vs. miR-NC + CCI-ION) (two-way ANOVA). (*E*) Intra-TG injection of antagomir-32-5p (antagomir-32)-induced mechanical pain hypersensitivity in intact rats (n = 8 to 10 rats per group). $^{*}P < 0.05$; $^{**}P < 0.01$ (vs. antagomir-NC, two-way ANOVA). (*F*) Intra-TG injection of miR-32-down in intact rats induced mechanical pain hypersensitivity (n = 7 to 9 rats per group). $^{*}P < 0.05$; $^{**}P < 0.01$ (vs. miR-NC, two-way ANOVA).

neurons using a neuron promoter-specific (human synapsin 1 gene promoter) combinatorial lentiviral vector lenti-hSyn-miR-32-5p-up (miR-32-up) containing enhanced green fluorescent protein (EGFP) as an expression marker. After direct injection of miR-32-up into intact TGs, EGFP expression was observed in injected TG neurons of all sizes after 3 d (Fig. 2*B*) and was maintained on day 21 (*SI Appendix*, Fig. S2*A*). qPCR analysis showed a consistent significant increase in miR-32-5p expression on day 3 after miR-32-up transduction (Fig. 2*B*). Intra-TG injection of miR-32-up 14 d after CCI-ION significantly relieved mechanical hyperalgesia on days 3 and 7 after miR-32-up transduction (Fig. 2*C*). Moreover, the role of miR-32-5p in neuropathic pain maintenance was further determined. We pretreated animals with miR-32-up before CCI-ION and then assessed the preventive effect of miR-32-5p overexpression on CCI-ION–induced mechanical allodynia. While overexpression of miR-32-5p by preinjection of miR-32-up did not affect nociceptive behaviors in sham-operated rats, treatment with miR-32-up dramatically alleviated mechanical allodynia in the rats on day 14 after CCI-ION (Fig. 2*D*).

Next, we also determined whether mimicking the nerve injury-induced down-regulation of miR-32-5p in the TG in intact rats alters nociceptive thresholds. Intra-TG injection of chemical-modified antagomir-32-5p produced mechanical hypersensitivity on the ipsilateral side (Fig. 2*E*). We further utilized a lentiviral short hairpin RNA-mediated miR-32-5p knockdown approach to evaluate the effect of miR-32-5p on nociceptive behavior. After intra-TG injection of lenti-hSyn-miR-32-5p-down (miR-32-down) into intact TGs, EGFP expression was observed on day 3, peaked on day 7, and was maintained on day 21 (*SI Appendix*, Fig. S2*B*). Consistent with the results of pharmacological inhibition, rats treated with miR-32-down, but not rats treated with lenti-hSyn-miR-32-5p-NC (miR-32-NC), showed the development of mechanical hypersensitivity (Fig. 2*F*). These effects occurred on day 3 and were maintained for at least 7 d after viral injection (Fig. 2*F*). Collectively, the behavioral results obtained by the different strategies suggest that miR-32-5p plays a pivotal role in the regulation of nociceptive behaviors.

Histone Methylation Induces miR-32-5p Down-Regulation in CCI-ION. How is miR-32-5p in the TG down-regulated after nerve injury? DNA methylation and histone modifications are considered to be the two major epigenetic mechanisms controlling gene expression (17). Interestingly, bioinformatic analysis with MethPrimer did not identify CpG islands in the miR-32-5p promoter region (*SI Appendix*, Fig. S3), excluding the possible involvement of DNA methylation in this regulatory mechanism.

Emerging evidence has suggested that histone modifications, mainly lysine acetylation and methylation, are implicated in miRNA regulation (18), and methylation at histone H3 lysine 9 (H3K9) and histone H3 lysine 27 (H3K27) have been shown to correlate strongly with transcriptional repression (19). We thus measured the activity of H3K9 dimethylation (H3K9me2) and H3K27 trimethylation (H3K27me3) after peripheral nerve injury. Immunoblot analysis revealed that CCI-ION induced a significant increase in the levels of H3K9me2 and H3K27me3 in the ipsilateral TG on day 14 post–CCI-ION compared to those in sham-operated rats (Fig. 3 *A* and *B* and *SI Appendix*, Fig. S4). Further examination of TG sections by FISH combined with immunostaining showed that H3K9me2 and H3K27me3 modifications colocalized with miR-32-5p in both sham-operated and CCI-ION rats (Fig. 3*C*). Notably, most of the TG neurons that had high levels of H3K9me2 and H3K27me3 expressed a modest level of miR-32 in injured TGs (Fig. 3*C*). Moreover, in both sham-operated and CCI-ION groups, H3K9me2 and H3K27me3 were primarily detected in the cell nuclei (labeled by DAPI) (Fig. 3*C*). In lysates from rat TGs, chromatin immunoprecipitation (ChIP) revealed that a fragment within the miR-32-5p gene promoter could be amplified from the complex immunoprecipitated with anti-H3K9me2 or anti-H3K27me3 antibodies in sham-operated rats (Fig. 3*D* and *SI Appendix*, Fig. S5), indicating the specific binding of H3K9me2 or H3K27me3 to the *miR-32-5p* gene. Furthermore, CCI-ION significantly increased the binding activity of H3K9me2 and H3K27me3, as shown by the respective 2.9-fold and 5.1-fold increases in the band density in the ipsilateral TG on day 14 post–CCI-ION compared to those in sham-operated rats (Fig. 3*E*). Next, we determined whether the increased H3K9me2 and H3K27me3 levels were involved in the mechanical allodynia observed on day 14 post–CCI-ION. Administration of UNC0638, a specific H3K9me2 inhibitor, significantly attenuated the CCI-ION–induced increase in H3K9me2 (Fig. 3*F* and *SI Appendix*, Fig. S6). Similar results were obtained with GSK503, a highly specific inhibitor of EZH2 (a chromatin-modifying enzyme), which significantly reduced the H3K27me3 level (Fig. 3*G* and *SI Appendix*, Fig. S7). Next, to examine the regulatory effects of H3K9me2 and H3K27me3 on miR-32-5p, we assessed the

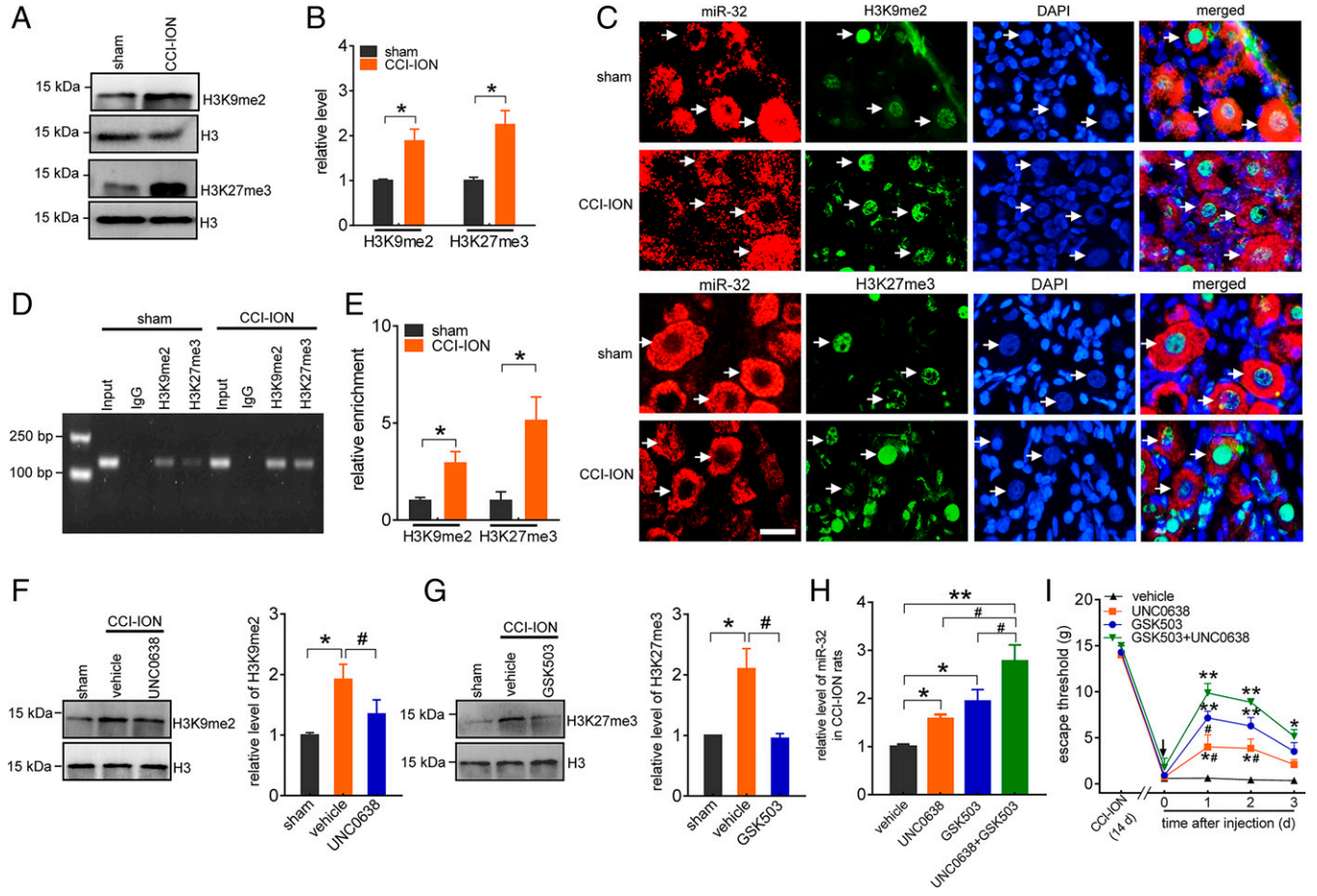

Fig. 3. Histone methylation induces miR-32-5p down-regulation in CCI-ION. (*A* and *B*) Representative immunoblots (*A*) and summary data (*B*) showing the protein-expression levels of H3K9me2 and H3K27me3 in TGs on day 14 after CCI-ION or sham operation. The immunoblots shown are representative of three independent experiments. H3 was used as a loading control. $^{*}P < 0.05$ (vs. sham, unpaired *t* test). (*C*) FISH combined with immunostaining of neurons labeled with DIG-labeled miR-32-5p probe (red), H3K9me2 or H3K27me3 proteins (green), and DAPI (blue) in rat TGs from the CCI-ION group compared to the sham-operated group, at day 14 postoperation. White arrows indicate colocalization. (Scar bar, 25 μm.) (*D* and *E*) Representative blots (*D*) and summary data (*E*) of ChIP-qPCR showing that the binding of H3K9me2 or H3K27me3 with miR-32-5p was increased after CCI-ION. Input, total purified fragments. Data were normalized to input and are presented as the mean ± SEM of at least triplicate experiments. $^{*}P < 0.05$ (vs. sham, unpaired *t* test). (*F* and *G*) The increased protein expression level of H3K9me2 (*F*) or H3K27me3 (*G*) in TGs on day 14 after CCI-ION was attenuated by UNC0638 (5 nmol) or GSK503 (5 nmol), respectively. $^{*}P < 0.05$ (vs. sham); $^{\#}P < 0.05$ (vs. vehicle) (one-way ANOVA). The immunoblots shown are representative of three independent experiments. (*H*) Effects of intra-TG injection of UNC0638 (5 nmol) and/or GSK503 (5 nmol) on the expression level of miR-32-5p in TGs on day 14 post–CCI-ION. Data are representative of three independent experiments performed in triplicate. $^{*}P < 0.05$; $^{**}P < 0.01$ (vs. vehicle); $^{\#}P < 0.05$ (vs. UNC0638 + GSK503) (one-way ANOVA). (*I*) Intra-TG injection of UNC0638 (5 nmol) and/or GSK503 (5 nmol) attenuated mechanical allodynia in rats on day 14 post–CCI-ION ($n = 8$ to 10 rats per group). $^{*}P < 0.05$; $^{**}P < 0.01$ (vs. vehicle); $^{\#}P < 0.05$ (vs. UNC0638 + GSK503) (two-way ANOVA).

expression of miR-32-5p after neuropathic pain induction and found that administration of UNC0638 or GSK503 significantly increased the level of miR-32-5p in the TG in rats on day 14 after CCI-ION (Fig. 3*H*). Notably, administration of both GSK503 and UNC0638 produced a significantly additive effect on the level of miR-32-5p compared to that of GSK503 or UNC0638 alone (Fig. 3*H*). Moreover, we assessed the roles of H3K9me2 and H3K27me3 in neuropathic pain in rats. Two weeks after CCI-ION, administration of UNC0638 partially attenuated mechanical allodynia. Similarly, a single injection of GSK503 significantly attenuated the decrease in the mechanical pain threshold 2 wk post–CCI-ION (Fig. 3*I*). Intriguingly, combination treatment with UNC0638 and GSK503 was more effective in suppressing mechanical allodynia than either agent alone in CCI-ION rats (Fig. 3*I*). Taken together, these findings suggest that nerve injury results in an increase in H3K9me2 and H3K27me3 modifications, thereby down-regulating the transcription of miR-32-5p and mediating trigeminal neuropathic pain.

Histone Methylation Decreases the Binding of GR to miR-32-5p. Histone methylation can regulate transcription by interfering with transcription factor binding (20). To identify the transcription factors that may regulate miR-32-5p expression, we used two computational algorithms, PROMO (http://alggen.lsi.upc.es) and Alibaba2.1, with a defined 80% profile score threshold and found that three transcription factors identified by both prediction algorithms—nuclear factor 1 (NF-1), CAAAT/enhancer binding protein beta (C/EBP beta), and the GR—had potential binding sites within the promoter region of miR-32-5p (Fig. 4*A*). To confirm the theoretical interaction between the miR-32-5p promoter region and these transcription factors, we subsequently constructed luciferase reporter plasmids carrying the wild-type miR-32-5p promoter sequence or sequences in the miR-32-5p promoter region containing mutations in the binding sites for these three transcription factors: mut-NF-1, mut-C/EBP$_\beta$, and mut-GR (Fig. 4*B*). Luciferase reporter assays revealed that expression of either mut-NF-1 or mut-C/EBP$_\beta$ caused a nonsignificant decrease in luciferase activity, while expression of mut-GR caused a significant decrease in luciferase activity (Fig. 4*C*). Further sequence-conservation analysis using the University of California, Santa Cruz Genome Browser showed that the binding site for GR is well conserved among mice, rats, and humans. FISH analysis of miR-32-5p combined with immunostaining for GR revealed endogenous GR expression in naïve rat TG neurons and indicated that GR was strongly colocalized with miR-32-5p (Fig. 4*D*). Immunostaining of GR demonstrated that GR was detected both in cytoplasm and in the cell nuclei (indicated by DAPI staining) (Fig. 4*D*). Thereafter, we determined whether this decrease in miR-32-5p expression was due to a change in the expression level of GR. Surprisingly, immunoblot analysis of TG lysates suggested that the protein expression of GR did not differ significantly between the sham-operated and CCI-ION groups (Fig. 4*E* and *SI Appendix*, Fig. S8). Histone modification might prevent transcription factors from binding promoter regions and participating in regulating miRNA expression (21). We then examined whether histone methylation affects the binding of GR to the promoter region of the *miR-32-5p* gene, resulting in decreased expression of miR-32-5p. In lysates from rat TGs, ChIP-PCR analysis indicated that a fragment within the miR-32-5p gene promoter could be amplified from the complex immunoprecipitated with an antibody specific for GR (Fig. 4*F* and *SI Appendix*, Fig. S9), but not from the complex immunoprecipitated with control IgG. Fourteen days after rats were subjected to CCI-ION, the binding of GR to the promoter region of

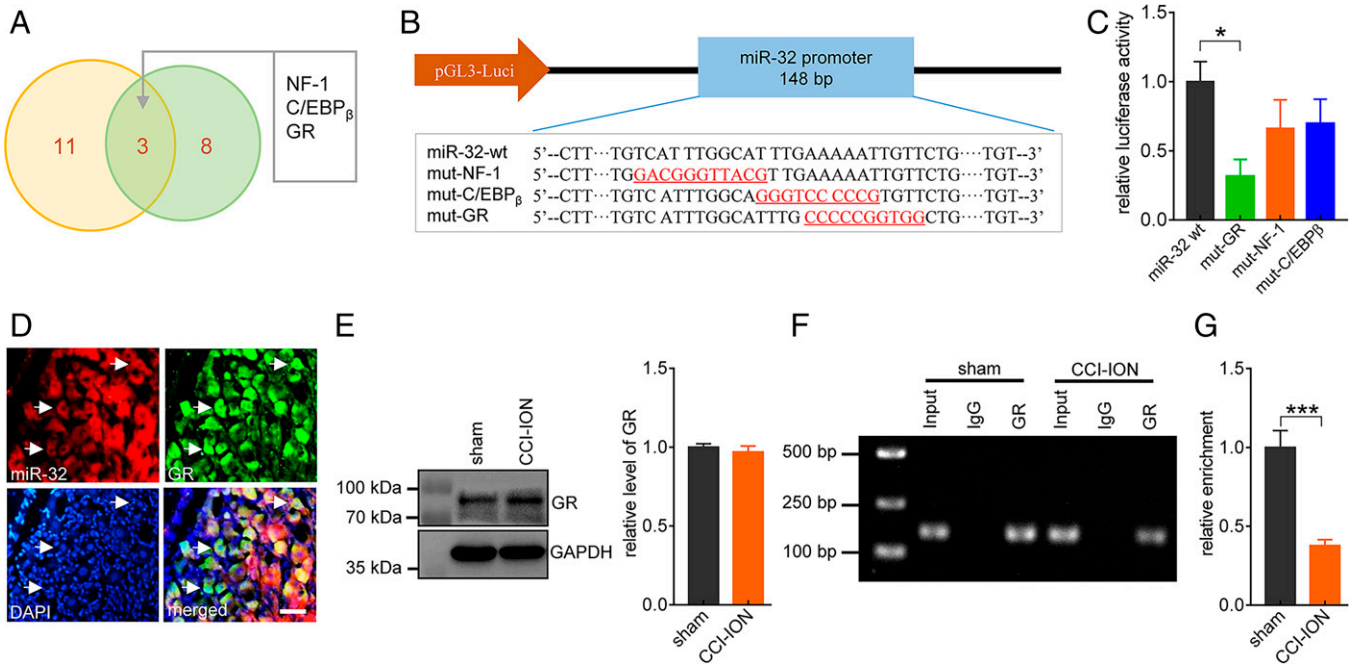

Fig. 4. Histone methylation decreases the binding of GR to miR-32-5p. (*A*) Venn diagrams showing that three transcription factors including NF-1, C/EBPβ, and GR were predicted to bind the miR-32-5p promoter by both the "PROMO" (green) and "Alibaba2.1" (yellow) algorithms. (*B*) Schematic diagrams showing luciferase reporter constructs carrying the wild-type (miR-32-wt) or mutant sequence in the miR-32-5p promoter region, including NF-1-binding sites (mut-NF-1), C/EBPβ-binding sites (mut-C/EBPβ), or GR-binding sites (mut-GR). (*C*) Dual-luciferase reporter activity assay with expression of miR-32-5p-wt, mut-NF-1, mut-C/EBP$_\beta$, or mut-GR. Data are representative of three independent experiments performed in triplicate. *$P < 0.05$ (vs. miR-32-wt, unpaired *t* test). (*D*) FISH combined with immunostaining analysis showing the colocalization of DIG-labeled miR-32-5p probe (red) with the GR protein (green) and DAPI (blue) in naïve rat TG sections. White arrows indicate colocalization. (Scale bar, 50 μm.) (*E*) Representative immunoblots and summary of the results showing the protein-expression level of GR in the ipsilateral TGs on day 14 after CCI-ION or sham operation. The immunoblots shown are representative of three independent experiments. (*F* and *G*) Representative blots (*F*) and summary data (*G*) of ChIP-qPCR showing that the binding of GR to the promoter region of the miR-32-5p gene was decreased after CCI-ION. Data are presented as the mean ± SEM of at least triplicate experiments. ***$P < 0.001$ (vs. sham, unpaired *t* test).

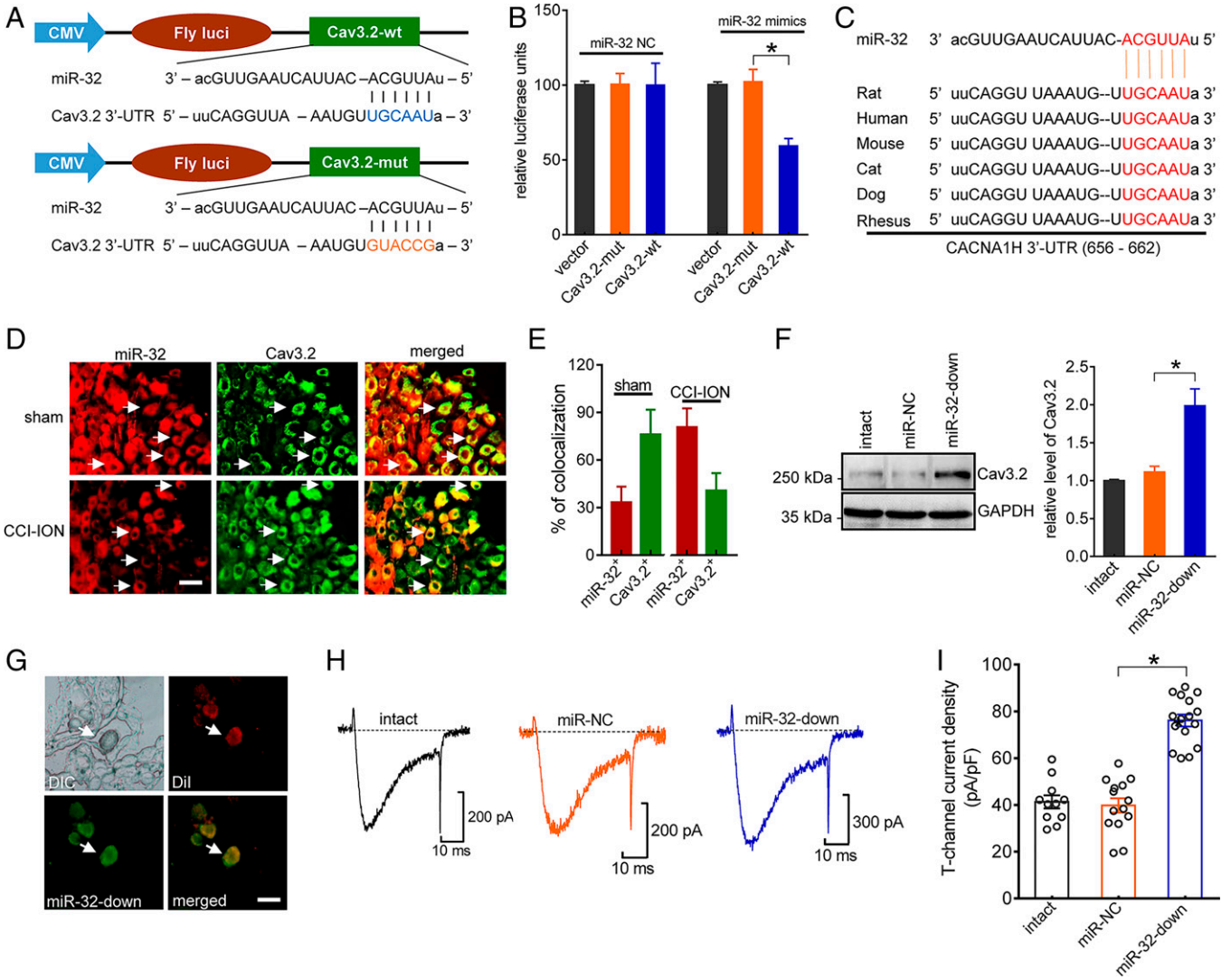

Fig. 5. miR-32-5p targets Ca^{2+} channels. (*A*) Schematic diagrams showing the luciferase reporter constructs carrying the wild-type (Cav3.2-wt) or mutant (Cav3.2-mut) Cav3.2 sequence. (*B*) Dual-luciferase reporter assay verifying the interaction between the 3′-UTR of Cav3.2 and miR-32-5p. Data are representative of three independent experiments. *$P < 0.05$ (vs. Cav3.2-mut, one-way ANOVA). (*C*) RNA sequences of the 3′-UTRs of Cav3.2 in various vertebrates, which are highly conserved and possess a conserved miR-32-5p–binding region. (*D*) FISH combined with immunostaining analysis showing the colocalization of DIG-labeled miR-32-5p probe (red) with Cav3.2 proteins (green) in TG sections of sham-operated and CCI-ION rats. White arrows indicate colocalization. (Scale bar, 50 μm.) (*E*) Summary of results showing the percentage of double-labeled neurons among miR-32-5p$^+$ or Cav3.2$^+$ neurons in sham-operated and CCI-ION groups. (*F*) Representative immunoblots (*Left*) and summary of results (*Right*) showing that knockdown of miR-32-5p by intra-TG injection of miR-32-down increased the protein expression of Cav3.2 in intact rats ($n = 7$ or 8 rats per group). *$P < 0.05$ (vs. miR-NC, one-way ANOVA). The immunoblots shown are representative of three independent experiments. (*G*) Representative images of retrograde DiI-labeled (red) TG neurons transduced with miR-32-down (green). (Scale bar, 50 μm.) (*H* and *I*) Representative current traces (*H*) and summary of the results (*I*) showing T-type channel currents recorded from both DiI-labeled and/or miR-32-down (or miR-NC)-transduced TG neurons in intact rats ($n = 11$ to 16 neurons per group). Knockdown of miR-32-5p significantly enhanced T-type channel current densities. *$P < 0.05$ (vs. miR-NC, one-way ANOVA).

miR-32-5p was significantly decreased (Fig. 4 *F* and *G*). Collectively, these results suggest that histone methylation attenuates the binding of GR to the promoter region of the *miR-32-5p* gene and decreases the expression level of miR-32-5p.

miR-32-5p Targets Ca^{2+} Channels. miRNAs inhibit the transcription of specific genes by binding to the 3′-UTR of their target mRNAs in a sequence-specific manner (6). We first used in silico algorithms TargetScan (http://www.targetscan.org) and miRDB (http://www.mirdb.org/) to screen for the potential targets of miR-32-5p in the context of trigeminal neuropathic pain. We made our focus on Cav3.2 channels among all the identified candidates because they are up-regulated in sensory neurons after nerve injury (22) and because silencing of Cav3.2 in dorsal root ganglion (DRG) neurons reduces the severity of neuropathic pain (23). Interestingly, miR-32-5p is also the miRNA that was predicted by both TargetScan and miRDB to regulate Cav3.2 mRNA. Therefore, the luciferase assays were used to verify whether Cav3.2 is a direct target of miR-32-5p. The predicted miR-32-5p–targeting sequence of Cav3.2 was cloned downstream of the firefly luciferase reporter gene (Fig. 5*A*). Indeed, miR-32-5p was able to robustly reduce the luciferase activity driven by the 3′-UTR of Cav3.2 (Fig. 5*B*). Such reduction was completely abolished when a mutation was introduced to the predicted seed sequence of Cav3.2 3′-UTR (Fig. 5*B*). This set of experiments clearly indicates that Cav3.2 is a direct target of miR-32-5p. It is worth noting that the miR-32-5p–binding site at the Cav3.2 3′-UTR is evolutionarily conserved among various vertebrates (Fig. 5*C*), suggesting that regulation of Cav3.2 by miR-32-5p is functionally important. We further examined whether miR-32-5p modulation affects the expression and function of Cav3.2 in TG neurons. FISH

coupled with immunostaining indicated that miR-32-5p was coexpressed with Cav3.2 in small- and medium-sized TG neurons of sham-operated rats (Fig. 5*D*). Image analysis indicated that 33.1% of miR-32-5p$^+$ neurons expressed Cav3.2, while 76.2% of Cav3.2$^+$ neurons expressed miR-32-5p (Fig. 5*E*). Compared to sham-operated counterparts, the ipsilateral TG neurons from CCI-ION rats expressed a lower level of miR-32-5p, but a higher level of Cav3.2 at 14 d after operation (Fig. 5 *D* and *E*). In injured TGs, 80.8% of miR-32-5p$^+$ neurons expressed Cav3.2, and 40.9% of Cav3.2$^+$ neurons expressed miR-32-5p (Fig. 5*E*). Intra-TG injection of miR-32-down, but not miR-32-NC, induced a significant increase in Cav3.2 protein expression in the TGs of intact rats (Fig. 5*F* and *SI Appendix*, Fig. S10). Moreover, whole-cell recording of small (soma diameter < 30 μm) TG neurons retrograde-labeled with DiI (Fig. 5*G*) indicated that knockdown of miR-32-5p significantly enhanced T-type channel currents (Fig. 5 *H* and *I*). Collectively, these results suggest that miR-32-5p directly targets the 3′-UTR of Cav3.2 to regulate the expression and function of Cav3.2 channels.

Cav3.2 Protein Expression Increases in TGs after CCI-ION. Next, we examined whether the protein expression of Cav3.2 is up-regulated in the context of neuropathic pain. On days 14, 21, and 28 after CCI-ION, the protein level of Cav3.2 was significantly increased in injured TGs, while neither Cav3.1 nor Cav3.3 exhibited a significant change in protein expression (Fig. 6 *A*–*C* and *SI Appendix*, Fig. S11). The increase in Cav3.2 protein expression was inversely correlated with miR-32-5p down-regulation (Fig. 6*D*). As expected, sham operation did not alter the basal protein expression of Cav3.2 in the ipsilateral TG after surgery (*SI Appendix*, Fig. S12). Additionally, the protein expression of Cav3.2 in the contralateral TG remained unchanged after CCI-ION (*SI Appendix*, Fig. S13). The Cav3.2 isoform is the major T-type channel isoform in peripheral nociceptors (24–27). Thus, we determined the expression pattern of Cav3.2. Immunostaining of intact rat TGs indicated that Cav3.2 was strongly colocalized with calcitonin gene-related peptide (CGRP) and isolectin B4-binding (IB_4), but showed comparatively little colocalization with 200-kDa neurofilament protein (NF200) (Fig. 6*E*). We further investigated whether the nerve injury-induced increase in Cav3.2 protein expression alters T-type channel currents, as well as the biophysical properties of small TG neurons retrograde-labeled with DiI (Fig. 6*F*). CCI-ION, but not sham operation, significantly increased the T-channel current density, and at −40 mV, the peak current density increased from 41.9 ± 6.2 to 83.3 ± 8.9 pA/pF (Fig. 6 *F* and *G*). Further evaluation of the biophysical properties of T-type channels showed that neither the voltage dependence of the activation properties (V_{half} from −43.1 ± 1.9 mV to −40.3 ± 2.7 mV; Fig. 6*H*) nor the half-maximal potential of steady-state inactivation (V_{half} from −69.5 ± 3.1 mV to −66.1 ± 2.8 mV; Fig. 6*I*) was significantly altered on day 14 post–CCI-ION compared to the corresponding values on day 14 post-sham operation. The functional significance of the T-type channels at the whole-animal level was further tested. Z941 (0.5 μM), an effective T-type channel blocker, robustly decreased T-type channel currents in small TG neurons in both the sham-operated and CCI-ION groups (Fig. 6*J*). Intra-TG injection of 2 nmol of Z941 attenuated the CCI-ION–induced decrease in the threshold for escape from mechanical stimulation (Fig. 6*K*). No difference in the basal mechanical responses of sham-operated rats was observed after intra-TG injection of either Z941 or vehicle (Fig. 6*K*). To further determine that the increased T-type channel currents by CCI-ION was due to Cav3.2 isoform specifically, we employed a small interfering RNA (siRNA)-mediated knockdown approach to silence Cav3.2 expression in injured TGs by using 6-carboxyfluorescein (6-FAM)–labeled chemically modified Cav3.2–siRNA. Our results showed that intra-TG injection of the Cav3.2 siRNA almost completely abolished the CCI-ION–induced increase in Cav3.2 protein expression (Fig. 6*L* and *SI Appendix*, Fig. S14). Administration of Cav3.2–siRNA markedly decreased T-type channel currents in small-sized TG neurons in both sham-operated and CCI-ION groups (Fig. 6 *M* and *N*).

Cav3.2 Is Responsible for miR-32-5p–mediated Neuropathic Analgesia. We determined whether modulation of miR-32-5p affects Cav3.2 protein expression in TGs after CCI-ION. First, we unilaterally injected the miRNA-32 mimic (agomir-32-5p) or the negative control agomir-NC into rat TGs. Administration of agomir-32-5p dramatically attenuated the increase in the protein expression of Cav3.2 on day 14 post–CCI-ION (Fig. 7*A* and *SI Appendix*, Fig. S15). Whole-cell recording of small TG neurons retrograde-labeled with DiI demonstrated that agomir-32-5p significantly attenuated the CCI-ION–induced increase in the T-type channel current density (Fig. 7 *B* and *C*). To obtain complementary support for this result, we induced miR-32-5p expression by intra-TG injection of miR-32-up into injured TGs. Expression of EGFP-labeled miR-32-5p via miR-32-up transduction was observed in TG neurons of various sizes (Fig. 2*B*), but was colocalized with Cav3.2 only in small and medium TG neurons (Fig. 7*D*). Statistical analysis showed that 85.7% of Cav3.2$^+$ neurons expressed miR-32-5p-up and that 35.9% of miR-32-5p-up$^+$ neurons expressed Cav3.2 (Fig. 7*D*). Immunoblot analysis showed that, compared with the robust protein expression of Cav3.2 in cells transduced with miR-32-NC, the protein expression of Cav3.2 was dramatically decreased in miR-32-up–transduced TG cells (Fig. 7*E* and *SI Appendix*, Fig. S16). Whole-cell recording of small TG neurons retrograde-labeled with DiI (Fig. 7*F*) demonstrated that overexpression of miR-32-5p significantly attenuated the CCI-ION–induced increase in the T-type channel current density (Fig. 7 *G* and *H*). Collectively, these results suggest that miR-32-5p and Cav3.2 are coexpressed in the same TG neurons and that reversing the nerve injury-induced down-regulation of miR-32-5p attenuates the expression and function of Cav3.2 channels. To further determine the role of Cav3.2 as mediator of miR-32-5p–induced analgesia, we induced miR-32-5p expression simultaneously with Cav3.2 silencing by siRNA in injured TGs of CCI-ION rats. The Cav3.2–siRNA was intra-TG–injected on day 0, and miR-32 was then administrated on day 3. Cav3.2 siRNA-treated (day 0) CCI-ION rats exhibited a significant decrease in mechanical allodynia compared with their negative control siRNA (NC-siRNA)-treated counterparts (Fig. 7*I*). Treatment with miR-32-up on day 3 had no further effect on mechanical sensitivity in Cav3.2 siRNA-treated CCI-ION rats, as evidenced by the stability of mechanical threshold recordings throughout the 3-d period after miR-32-5p-up administration (Fig. 7*I*), suggesting that miR-32-5p and Cav3.2 siRNA likely share the same cellular signaling pathway in vivo. In addition, NC-siRNA–treated CCI-ION rats responded to miR-32-up (Fig. 7*I*), similar to rats that did not receive siRNA (Fig. 2*C*), in which miR-32-up treatment induced a significant increase in the mechanical pain threshold (Fig. 7*I*).

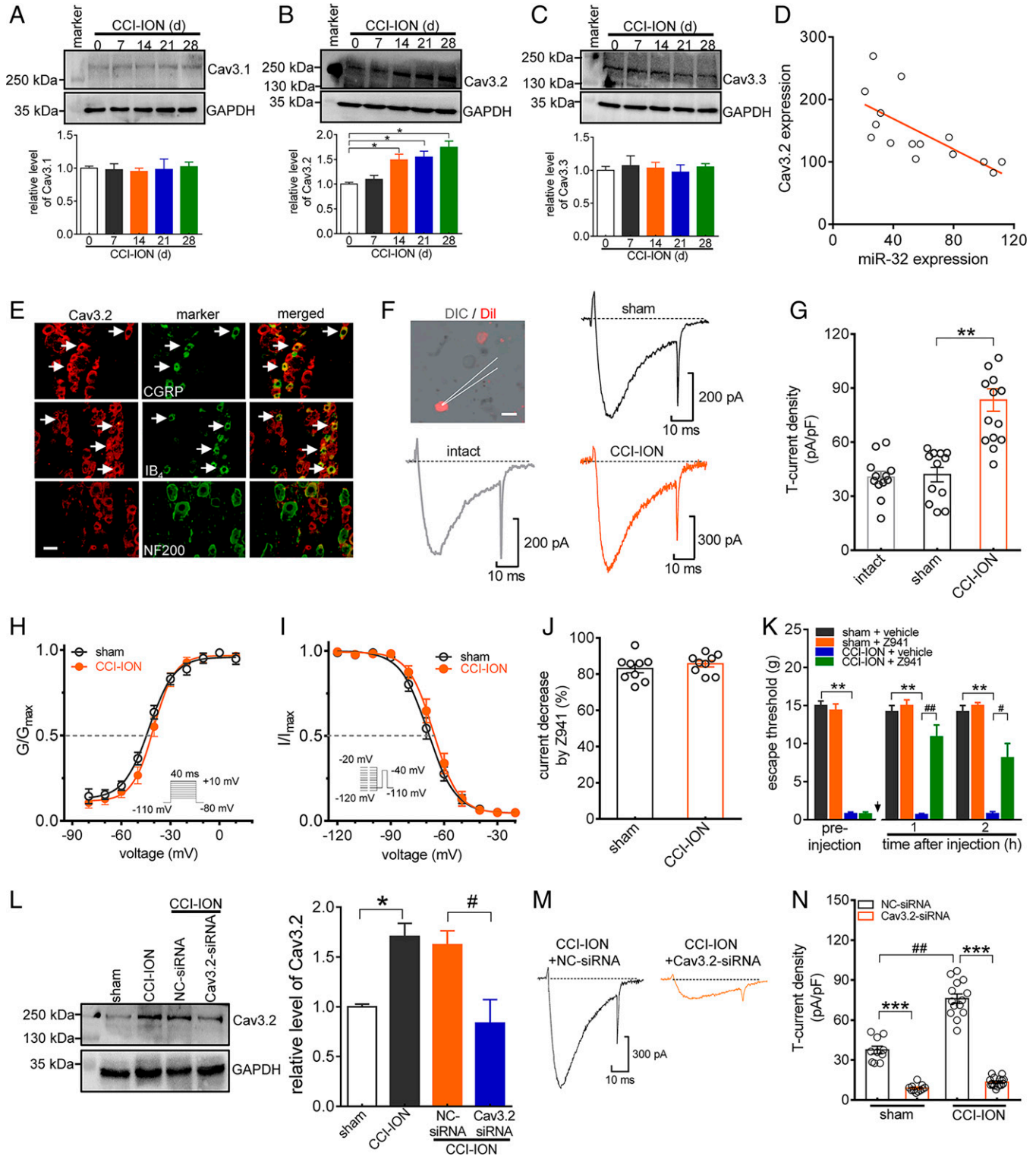

Fig. 6. Cav3.2 protein increases in TGs after CCI-ION. (*A–C*) Protein expression levels of Cav3.1 (*A*), Cav3.2 (*B*), and Cav3.3 (*C*) in rat TGs on days 0, 7, 14, 21, and 28 post–CCI-ION. $^{*}P < 0.05$ (vs. control [0 d], one-way ANOVA). Depicted immunoblots are representative of three independent experiments. (*D*) Linear regression analysis showed that the miR-32-5p level was inversely related to the Cav3.2 expression level in the ipsilateral TGs ($R^2 = 0.4805$). (*E*) Representative images of double immunostaining of Cav3.2 with CGPR, IB_4, and NF200 in rat TG sections. White arrows indicate double-labeled neurons. (Scale bar, 50 μm.) (*F*) Representative current traces of T-type channel currents recorded from retrograde DiI-labeled small TG neurons on day 14 post–CCI-ION or after sham operation. (*F, Inset*) Recording from a DiI-labeled TG neuron. (Scale bar, 50 μm.) (*G*) Summary of results showing the T-type channel current density in small TG neurons on day 14 post–CCI-ION or after sham operation ($n = 12$ to 15 neurons per group). No significant changes were observed between the intact and sham-operated groups. $^{**}P < 0.01$ (vs. sham, one-way ANOVA). (*H* and *I*) Nerve injury induced by CCI-ION (14 d) did not affect voltage-dependent activation ($n = 12$ neurons per group; *H*) or the steady-state inactivation profile ($n = 15$ neurons per group; *I*) of T-type channels. *H* and *I*, *Insets* indicate stimulation protocols. (*J*) Application of Z941 at 0.5 μM dramatically decreased T-type channel currents in TG neurons on day 14 post–CCI-ION ($n = 9$ neurons per group) or after sham operation ($n = 8$ neurons per group). (*K*) Intra-TG injection of Z941 (2 nmol) alleviated mechanical allodynia on day 14 post–CCI-ION. $n = 8$ to 11 rats per group. $^{**}P < 0.01$ (vs. vehicle + sham); $^{\#}P < 0.05$; $^{\#\#}P < 0.01$ (vs. CCI-ION + vehicle) (two-way ANOVA). (*L*) Intra-TG injection of Cav3.2 siRNA (Cav3.2-siRNA) attenuated the increased protein expression of Cav3.2 in the ipsilateral TGs on day 14 post–CCI-ION. $n = 7$ or 8 rats per group. $^{*}P < 0.05$ (vs. sham); $^{\#}P < 0.05$ (vs. CCI-ION + NC-siRNA) (one-way ANOVA). The immunoblots shown are representative of three independent experiments. (*M*) Representative current traces of T-type channel currents recorded from retrograde DiI-labeled small TG neurons on day 14 post–CCI-ION. (*N*) Summary of results showing the T-type channel current density in small TG neurons on day 14 post–CCI-ION or after sham operation ($n = 10$ to 16 neurons per group). $^{***}P < 0.001$ (vs. NC-siRNA); $^{\#\#}P < 0.01$ (vs. NC-siRNA + sham) (one-way ANOVA).

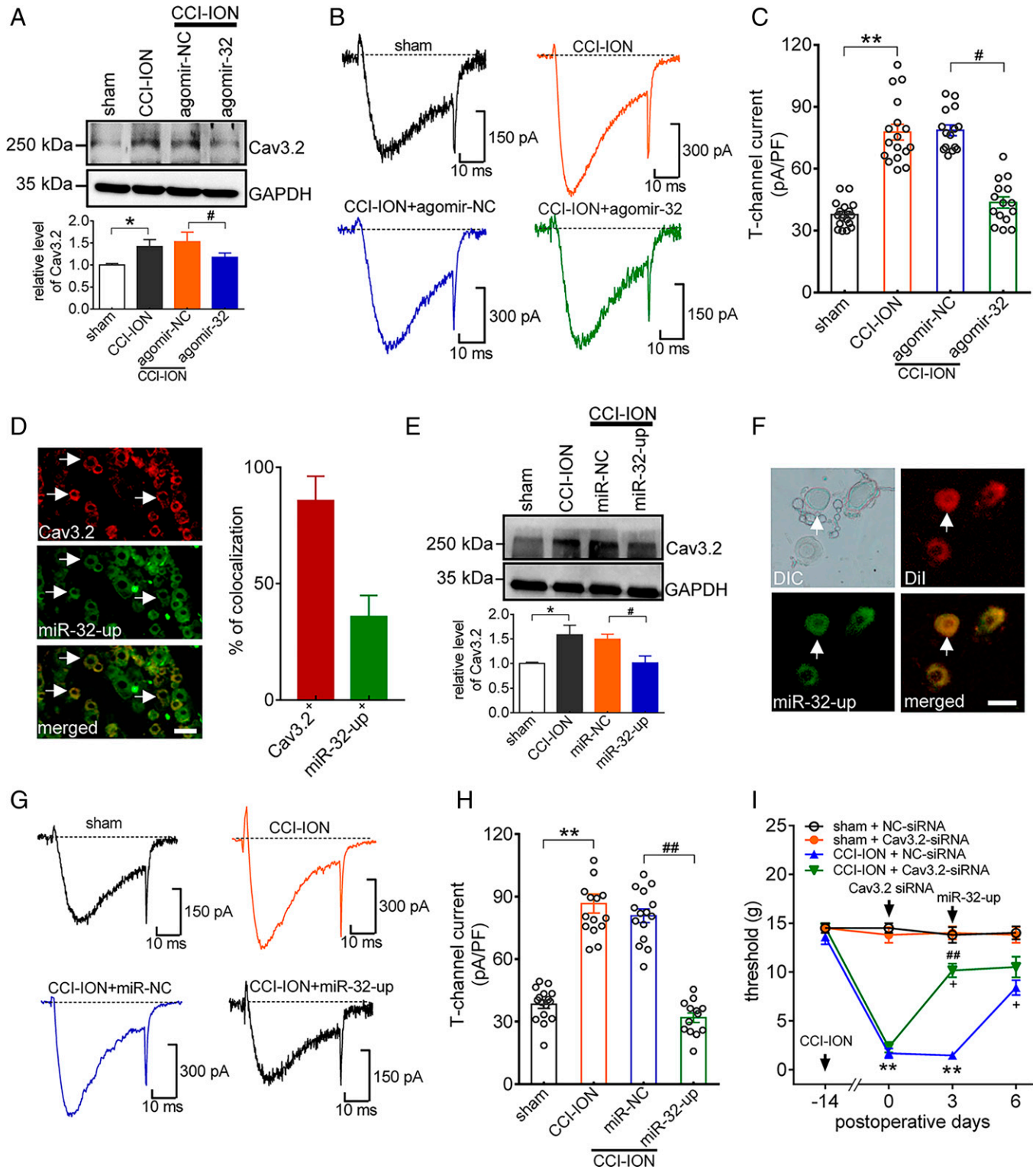

Fig. 7. Cav3.2 is responsible for miR-32-5p–mediated analgesia of neuropathic pain. (*A*) Western blot analysis showed that the increased expression level of Cav3.2 in the ipsilateral TGs on day 14 post–CCI-ION was attenuated by intra-TG injection of agomir-32-5p. $^{*}P < 0.05$ (vs. sham); $^{\#}P < 0.05$ (vs. CCI-ION + agomir-NC) (one-way ANOVA). The immunoblots shown are representative of three independent experiments. (*B* and *C*) Representative current traces (*B*) and summary of the results (*C*) for T-type channel currents recorded from both DiI-labeled and/or agomir-32-5p (or agomir-NC)-transduced TG neurons on day 14 post–CCI-ION or after sham operation ($n = 12$ to 17 neurons per group). $^{**}P < 0.01$ (vs. sham); $^{\#}P < 0.01$ (vs. CCI-ION + agomir-NC) (one-way ANOVA). (*D*, *Left*) Immunostaining analysis showing the colocalization of miR-32-5p with the Cav3.2 protein in an intact TG 3 d after injection of a miR-32-up. White arrows indicate colocalization. (Scale bar, 50 μm.) (*D*, *Right*) Summary of the results showing the percentage of double-labeled neurons among miR-32-up–transduced neurons or $Cav3.2^{+}$ neurons. (*E*) Intra-TG injection of miR-32-up attenuated the increased protein expression of Cav3.2 in the ipsilateral TGs on day 14 post–CCI-ION. $n = 7$ or 8 rats per group. $^{*}P < 0.05$ (vs. sham); $^{\#}P < 0.05$ (vs. CCI-ION + miR-NC) (one-way ANOVA). The immunoblots shown are representative of three independent experiments. (*F*) Representative images of retrograde DiI-labeled (red) TG neurons transduced with miR-32-up (green). (Scale bar, 50 μm.) (*G* and *H*) Representative current traces (*G*) and summary of the results (*H*) for T-type channel currents recorded from both DiI-labeled and/or miR-32-up (or miR-NC)-transduced TG neurons on day 14 post–CCI-ION or after sham operation ($n = 12$ to 15 neurons per group). $^{**}P < 0.01$ (vs. sham); $^{\#\#}P < 0.01$ (vs. CCI-ION + miR-NC) (one-way ANOVA). (*I*) Effect of siRNA-mediated knockdown of Cav3.2 (day 0) vs. negative control (NC-siRNA) on miR-32-up (intra-TG injection on day 3)–induced alleviation of mechanical allodynia in CCI-ION rats. $^{**}P < 0.01$ (vs. NC-siRNA + sham); $^{\#\#}P < 0.01$ (vs. CCI-ION + Cav3.2-siRNA at day 0); $^{+}P < 0.05$ (vs. CCI-ION + NC-siRNA at day 3) (two-way ANOVA).

Discussion

In this study, we identified miR-32-5p as a key functional noncoding RNA in contributing to neuropathic pain. miR-32-5p down-regulation appears causally involved in trigeminal neuropathic pain, and exogenous miR-32-5p specifically and effectively alleviates nociceptive behavior. Moreover, miR-32-5p targets the expression of Cav3.2 T-type channels. Histone methylation attenuates the binding of GR to the promoter region of the *miR-32-5p* gene and decreases the expression of miR-32-5p, in turn promoting the development of neuropathic pain through regulation of Cav3.2 channels (Fig. 8). As such, miR-32-5p–mediated translational regulation of Cav3.2 channels has a profound impact on the pathophysiology of chronic neuropathic pain, at molecular, cellular, and functional levels. Replenishment of miR-32-5p offers opportunity for the management of chronic neuropathic pain.

miRNAs are small noncoding RNAs that inhibit the transcription of target genes by binding to the 3′-UTR of target mRNAs (6, 28). Although accumulating molecular and functional evidence supports the alteration of miRNA expression in different nerve tissues under different pain conditions, little is known as to how miRNA expression itself is regulated during these processes. Two major epigenetic mechanisms have been shown to be involved in gene expression: DNA methylation and histone modification (29). In this study, no CpG islands were identified in the miR-32-5p promoter region. We showed that CCI-ION significantly increased the occupancy of two repressive histone marks, H3K27me3 and H3K9me2, and that these modifications participated in the regulation of trigeminal neuropathic pain in rats. Histone methylation might prevent GR from binding to the miR-32-5p promoter region and mediate a decrease in miR-32-5p expression. It is known that activated glucocorticoid (GC)-GR protein dimers translocate into the nucleus to regulate their target genes and ultimately modify pain-related protein expression (30). Neuropathic pain induced by nerve injury, which is usually accompanied by stress, might affect the GC release (31). Therefore, hormones that compromise the physiological response to stress (e.g., GC) may interact with effectors of neuropathic pain (32) and regulate pain-like behaviors (33). In addition, consistent with our present findings, a previous study showed that spinal nerve ligation increased the levels of H3K9me2 and H3K27me3 in rat DRGs. Interestingly, in the same study, H3K9me2, but not H3K27me3, inhibited the expression of potassium channels and was found to play a pivotal role in nociception (34). Although this discrepancy requires further investigation, histone modifications associated with transcriptionally inactive chromatin might vary in different tissue/cell types expressing distinct dimethyltransferases and/or demethylases in different neuropathic pain models. For example, increased H3K9me2 occupancy at promoters mediated through the G9a/GLP histone lysine dimethyltransferase generally mediates transcriptional repression and gene silencing (35), while H3K27me3 modification is mediated through polycomb group proteins (36). Moreover, emerging evidence suggests that the balance between acetylation and methylation of H3K9 or H3K27 contributes to gene transcription (37). While lysine acetylation can relax chromatin and enhance transcriptional activation, lysine methylation can cause different effects on gene expression, depending upon position (18). For instance, methylation at K4, K36, and K79 of H3 is associated with gene activation, whereas methylation at K9 and K27 of H3 correlates with transcriptional repression (19). Although beyond the scope of the current study, there is a strong possibility that combined changes in histone modification (i.e., decreased H3K9ac and increased H3K9me2/H3K27me3 occupancy) affect the binding of GR to the *miR-32-5p* gene promoter in the injured TG. Furthermore, in-silicon prediction by the Alibaba2 algorithm indicates a 5-repeated-nucleotide overlap between the C/EBP$_\beta$ binding site and the GR binding site at the promoter region of the *miR-32-5p* gene. However, transfection of mut-C/EBP$_\beta$–expressing vectors has no effect on the promoter luciferase activity, ruling out the involvement of C/EBP$_\beta$ in initiating miR-32-5p transcription. Indeed, further prediction with the PROMO algorithm suggested a multiple discontinuous binding motif for C/EBP$_\beta$ (TTG) and GR (TGT) in the promoter region of the *miR-32-5p* gene. Interestingly, previous studies have shown that in DRG neurons the binding site of C/EBP$_\beta$ in the promoter region of the *Ehmt2* gene (attgcgcagt) also contained TTG sequence (38), while in hippocampus, the GR binding motif in the promoter region of the *Adra1d* gene (gaacggcctgtacc) contained TGT (39). Thus, the TGT sequence is critical for GR binding, although it may not be the only determinant.

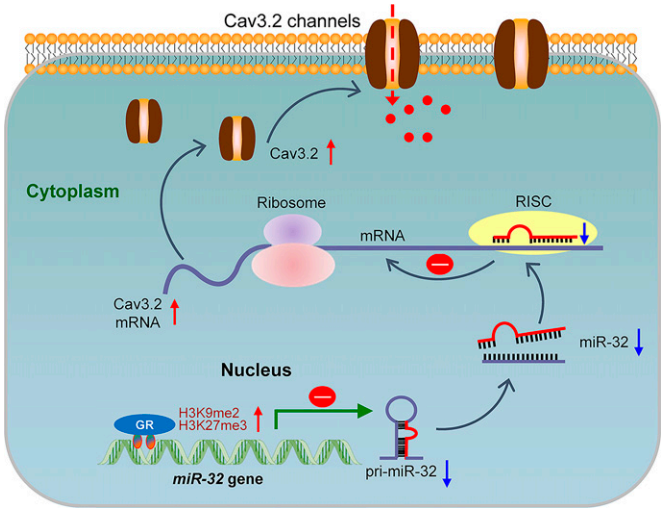

Fig. 8. Proposed mechanism by which miR-32-5p participates in neuropathic pain. Nerve injury increases the occupancy of H3K9me2 and H3K27me3 at the miR-32-5p promoter region in rat TG neurons, resulting in the decreased binding of GR and leading to a decrease in the expression of miR-32-5p. The RNA-induced silencing complex (RISC) guides mature single-stranded miR-32-5p to its target sequence within the 3′-UTR of the mRNA of the α1 subunit of Cav3.2, resulting in degradation of the mRNA. The down-regulation of miR-32-5p in nerve injury causes increases Cav3.2 protein expression, which results in enhanced T-type channel currents in TG neurons and produces mechanical neuropathic pain symptoms in rats.

Cav3.2 is the predominant T-type channel isoform expressed at the soma of sensory neurons and is responsible primarily for subthreshold neuronal excitability and modulation of nociceptive behaviors (23, 24, 40). Our findings indicate that TG neurons express both miR-32-5p and Cav3.2 and that Cav3.2 protein expression is increased in TG neurons with reduced miR-32-5p levels. TG neurons immunoreactive for Cav3.2 were mainly labeled with IB$_4$ and CGRP, while few Cav3.2-labeled TG neurons coexpressed NF200. This expression pattern is consistent with previous data showing abundant expression of Cav3.2 channels in small- to medium-sized TG neurons (25, 41), while distinct from the broader distribution of Cav3.2 in rat DRG neurons (42). Cav3.2 channels were reported to be expressed exclusively in small DRG neurons in naïve mice (43, 44); however, these results seem to be contradictory to those of most related studies. Increased expression of Cav3 isoform T-type channels in sensory neurons has shown functional diversity in distinct pain disorders (23, 45, 46). For instance, Cav3.2 expression is significantly enhanced in DRGs of injured animals (22, 26, 27, 47). However, in a neuropathic pain model induced by paclitaxel, Cav3.2 expression is not

necessarily elevated (48). Furthermore, spinal nerve injury was reported to increase Cav3.2 and Cav3.3 mRNA levels in rat DRGs, whereas Cav3.1 mRNA was not detected (49). Interestingly, in mice with carrageenan-induced inflammatory hyperalgesia, the expression of Cav3.2 mRNA, but not Cav3.1 or Cav3.3 mRNAs, was up-regulated in ipsilateral DRG neurons (44). In contrast, an increased level of Cav3.3 mRNA in mouse sensory neurons was implicated to participate in pain modulation (50). In this study involving rats, we found that all three Cav3 isoforms were expressed in TGs and that nerve injury induced by CCI-ION triggered the selective increase in Cav3.2 expression at both the mRNA and protein levels, with no significant changes in Cav3.1 or Cav3.3 expression observed. This was further confirmed by the findings that intra-TG injection of Cav3.2 siRNA significantly alleviated mechanical allodynia induced by CCI-ION. Consistent with our findings, the selective inhibition of Cav3.2 channels reversed the hyperexcitability of peripheral nociceptors and alleviated postsurgical pain (24). The effects of silencing Cav3.2 channels in peripheral sensory neurons have previously demonstrated a critical role for these channels in nociception (23). However, loss of T-type channels may also contribute to decreased spike-frequency adaptation and increased excitability after injury to sensory neurons (51). In this study, T-type channel currents were recorded mainly in medium-sized neurons, indicating that neuron size might be a critical factor that led to this discrepancy. Moreover, it should be noted that while nociceptors in peripheral tissues, including the TG and DRG, show a high degree of functional similarity, there are important differences in their developmental lineages, and recent genome-wide gene-expression analyses suggest that they possess unique signatures (4, 5, 52). Although we have demonstrated the importance of miR-32-5p–mediated targeting of Cav3.2 channel expression in regulating trigeminal neuropathic pain, Cav3.2 may not be the only factor involved in miR-32-5p–mediated mechanical allodynia. miR-32-5p is reported to regulate the expression of a variety of genes. For instance, miR-32-5p influences high-glucose-induced cardiac fibroblast proliferation by inhibiting DUSP1 (13) and cell-cycle progression via PTEN up-regulation in bone marrow-derived mesenchymal stem cells (14). Moreover, miR-32-5p promotes lipid metabolism in oligodendrocytes and increases myelin production through the regulation of its target SLC45A3 (15). These findings suggest that miR-32-5p can effectively and cooperatively regulate many aspects of physiological and/or pathological processes. Further insight into the function of miR-32-5p in neurons will improve our understanding of the pathophysiology of neuropathic pain.

In summary, the present study offers insights into the epigenetic mechanisms of miR-32-5p involved in transcriptional *Cav3.2* gene silencing in trigeminal neuropathic pain. We report that nerve injury caused substantial and persistent Cav3.2 channel up-regulation in rat TGs. Increased Cav3.2 expression induced by nerve injury was associated with altered histone methylation and GR binding to the miR-32-5p promoter region, which in turn caused mechanical allodynia. Overall, the identification of the role of miRNA-32 in regulating Cav3.2 channels in the context of trigeminal-driven pain may provide potential targets to prevent and treat neuropathic pain conditions.

Materials and Methods

Detailed descriptions of methods and materials are provided in *SI Appendix, SI Materials and Methods*.

Animal Model. All experimental procedures performed in this study were carried out in accordance with NIH guidelines and had been approved by the Institutional Animal Care and Use Committee of Soochow University. Every effort was made to minimize the number of animals used and animal suffering. Animals (Sprague–Dawley rats, 140 to 160 g, male) were housed under a standard 12/12-h light–dark cycle in a temperature- and humidity-controlled room with food and water provided ad libitum. A trigeminal neuropathic pain model was produced by CCI-ION via an intraoral approach, as described in previous studies (53–55) with some modifications.

Behavioral Tests and Drug Application. All behavioral experiments were carried out with the investigators blinded to treatment conditions. Orofacial behavioral tests as described by Vos et al. (56) were performed 1 d before and at designated times after CCI-ION surgeries. Orofacial response threshold of mechanical sensitivity was determined as described (25, 57). The 5′-cholesteryl–modified and 2′-*O*-methyl–modified siRNA for Cav3.2 (Cav3.2–siRNA), agomir-32-5p, antagomir-32-5p, or relevant scrambled controls (RiboBio Biological Technology), labeled with 6-FAM, were diluted to a concentration of 50 μM in diethyl pyrocarbonate H_2O.

Western Blot Analysis. Western blot analysis was performed as described (25, 27).

Real-Time qPCR. Total RNA was extracted from the TG tissues by using RNAiso Plus (Takara). According to the protocol provided by the manufacturer of the Hairpin-it MicroRNA Quantitation PCR kit (GenePharma), 1 μg of RNA was reverse-transcribed to complementary DNA (cDNA).

Immunofluorescence Staining. Immunostaining was conducted as described (25, 27).

FISH. Locked nucleic acid (LNA)–digoxin (DIG)-labeled probes specific for miR-32-5p (rno-miR-32-5p miRCURY LNA detection probe, 5′-digoxin–TGCAACTTAG-TAATGTGCAATA–digoxin-3′) and negative control probes were obtained from Exon.

Luciferase Reporter Assay. The mRNA for the full-length 3′-UTR of Cav3.2 was amplified by PCR from rat cDNA. Plasmids encoding firefly luciferase followed by the wild-type Cav3.2 3′-UTR (Cav3.2-wt) or mutant Cav3.2 3′-UTR (Cav3.2-mut) were constructed. Sequences of the miR-32-5p promotor region with mutant binding sites for NF-1, C/EBPβ, or GR were constructed and inserted into the pGL3 plasmid.

ChIP-PCR. ChIP-enriched DNA was analyzed by qPCR using the following ChIP primers: forward, 5′-CTTTTCTCCTCACTCCTGCTCA-3′; and reverse, 5′-ACACTCC-CAACCTGGAATCTTT-3′.

Dissociation of TG Neurons. TG neurons were dissociated as described in our previous studies (25).

Electrophysiology. Whole-cell patch-clamp recordings were carried out as described in our previous studies (25, 27).

Data Analysis and Statistics. Values are reported as the mean ± SEM. Data acquisition and statistical analysis were performed by using ClampFit 10.2 (Molecular Devices), Prism 6.0 (GraphPad Software), and Microsoft Excel. Plots showing voltage-dependent activation and steady-state inactivation were fitted by the Boltzmann equation. Statistical comparisons of several groups were performed by using one-way ANOVA and subsequent Bonferroni correction, if not stated otherwise. The paired or unpaired *t* test was used to compare two groups as appropriate. The behavioral data were analyzed by two-way repeated-measures ANOVA with a post hoc Bonferroni test. Differences with $P < 0.05$ were considered to be statistically significant.

Data Availability. The raw sequencing data have been deposited in the National Center for Biotechnology Information Gene Expression Omnibus (accession no. GSE192803) (58). All other study data are included in the article and *SI Appendix*.

ACKNOWLEDGMENTS. We thank Mrs. Shan Gong and Dr. Heyi Ji for their technical assistance. This study was supported by National Natural Science Foundation of China Grants 82071236, 81873731, 81771187, and 31800879; Natural Science Foundation of Colleges and Universities in Jiangsu Province Grant 19KJA210003; Natural Science Foundation of Jiangsu Province Grant BK20211073; Research Innovation Program for College Graduates of Jiangsu Province Grant KYCX21_2965; Science and Technology Bureau of Suzhou Grant

SYS2020129; Jiangsu Key Laboratory of Neuropsychiatric Diseases Grant BM2013003; and a project funded by the Priority Academic Program Development of Jiangsu Higher Education Institutions. T.P.S. is supported by Canadian Institutes of Health Research Grant 10677.

Author affiliations: [a]Department of Physiology and Neurobiology, Medical College of Soochow University, Suzhou 215123, People's Republic of China; [b]Centre for Ion Channelopathy, Medical College of Soochow University, Suzhou 215123, People's Republic of China; [c]Jiangsu Province Key Laboratory of Anesthesiology, Xuzhou Medical University, Xuzhou 221004, People's Republic of China; [d]Jiangsu Key Laboratory of Neuropsychiatric Diseases, Soochow University, Suzhou 215123, People's Republic of China; [e]Institute of Regenerative Biology and Medicine, Helmholtz Zentrum München, München 81377, Germany; [f]Michael Smith Laboratories, University of British Columbia, Vancouver, BC V6T 1Z4, Canada; [g]Djavad Mowafaghian Centre for Brain Health, University of British Columbia, Vancouver, BC V6T 1Z4, Canada; [h]Department of Geriatrics, The Second Affiliated Hospital of Soochow University, Suzhou 215004, People's Republic of China; and [i]Clinical Research Center of Neurological Disease, The Second Affiliated Hospital of Soochow University, Suzhou 215004, People's Republic of China

1. R. R. Ji, G. Strichartz, Cell signaling and the genesis of neuropathic pain. *Sci. STKE* **2004**, reE14 (2004).
2. A. B. O'Connor, R. H. Dworkin, Treatment of neuropathic pain: An overview of recent guidelines. *Am. J. Med.* **122** (10 suppl.), S22–S32 (2009).
3. K. Fried, U. Bongenhielm, F. M. Boissonade, P. P. Robinson, Nerve injury-induced pain in the trigeminal system. *Neuroscientist* **7**, 155–165 (2001).
4. O. A. Korczeniewska *et al.*, Differential gene expression changes in the dorsal root versus trigeminal ganglia following peripheral nerve injury in rats. *Eur. J. Pain* **24**, 967–982 (2020).
5. S. Megat *et al.*, Differences between dorsal root and trigeminal ganglion nociceptors in mice revealed by translational profiling. *J. Neurosci.* **39**, 6829–6847 (2019).
6. D. P. Bartel, MicroRNAs: Target recognition and regulatory functions. *Cell* **136**, 215–233 (2009).
7. R. Rupaimoole, F. J. Slack, MicroRNA therapeutics: Towards a new era for the management of cancer and other diseases. *Nat. Rev. Drug Discov.* **16**, 203–222 (2017).
8. B. John *et al.*, Human microRNA targets. *PLoS Biol.* **2**, e363 (2004).
9. B. M. Lutz, A. Bekker, Y. X. Tao, Noncoding RNAs: New players in chronic pain. *Anesthesiology* **121**, 409–417 (2014).
10. G. Bai, R. Ambalavanar, D. Wei, D. Dessem, Downregulation of selective microRNAs in trigeminal ganglion neurons following inflammatory muscle pain. *Mol. Pain* **3**, 15 (2007).
11. R. Ng *et al.*, miRNA-32 drives brown fat thermogenesis and trans-activates subcutaneous white fat browning in mice. *Cell Rep.* **19**, 1229–1246 (2017).
12. Y. Wang *et al.*, CUL4B renders breast cancer cells tamoxifen-resistant via miR-32-5p/ER-α36 axis. *J. Pathol.* **254**, 185–198 (2021).
13. J. Shen *et al.*, MiR-32-5p influences high glucose-induced cardiac fibroblast proliferation and phenotypic alteration by inhibiting DUSP1. *BMC Mol. Biol.* **20**, 21 (2019).
14. G. Zhu, J. Chai, L. Ma, H. Duan, H. Zhang, Downregulated microRNA-32 expression induced by high glucose inhibits cell cycle progression via PTEN upregulation and Akt inactivation in bone marrow-derived mesenchymal stem cells. *Biochem. Biophys. Res. Commun.* **433**, 526–531 (2013).
15. D. Shin, S. Y. Howng, L. J. Ptáček, Y. H. Fu, miR-32 and its target SLC45A3 regulate the lipid metabolism of oligodendrocytes and myelin. *Neuroscience* **213**, 29–37 (2012).
16. E. Cheong, H. S. Shin, T-type Ca2+ channels in normal and abnormal brain functions. *Physiol. Rev.* **93**, 961–992 (2013).
17. R. Jaenisch, A. Bird, Epigenetic regulation of gene expression: How the genome integrates intrinsic and environmental signals. *Nat. Genet.* **33** (suppl.), 245–254 (2003).
18. S. Morales, M. Monzo, A. Navarro, Epigenetic regulation mechanisms of microRNA expression. *Biomol. Concepts* **8**, 203–212 (2017).
19. M. T. McCabe, J. C. Brandes, P. M. Vertino, Cancer DNA methylation: Molecular mechanisms and clinical implications. *Clin. Cancer Res.* **15**, 3927–3937 (2009).
20. T. Kouzarides, Histone methylation in transcriptional control. *Curr. Opin. Genet. Dev.* **12**, 198–209 (2002).
21. Q. Yao, Y. Chen, X. Zhou, The roles of microRNAs in epigenetic regulation. *Curr. Opin. Chem. Biol.* **51**, 11–17 (2019).
22. X. J. Kang *et al.*, Increased expression of $Ca_V3.2$ T-type calcium channels in damaged DRG neurons contributes to neuropathic pain in rats with spared nerve injury. *Mol. Pain* **14**, 1744806918765808 (2018).
23. E. Bourinet *et al.*, Silencing of the Cav3.2 T-type calcium channel gene in sensory neurons demonstrates its major role in nociception. *EMBO J.* **24**, 315–324 (2005).
24. S. L. Joksimovic *et al.*, Selective inhibition of $Ca_V3.2$ channels reverses hyperexcitability of peripheral nociceptors and alleviates postsurgical pain. *Sci. Signal.* **11**, eaao4425 (2018).
25. H. Wang *et al.*, Brain-derived neurotrophic factor stimulation of T-type Ca^{2+} channels in sensory neurons contributes to increased peripheral pain sensitivity. *Sci. Signal.* **12**, eaaw2300 (2019).
26. Y. Li *et al.*, Dorsal root ganglion neurons become hyperexcitable and increase expression of voltage-gated T-type calcium channels (Cav3.2) in paclitaxel-induced peripheral neuropathy. *Pain* **158**, 417–429 (2017).
27. Y. Zhang *et al.*, Peripheral pain is enhanced by insulin-like growth factor 1 through a G protein-mediated stimulation of T-type calcium channels. *Sci. Signal.* **7**, ra94 (2014).
28. S. M. Eacker, T. M. Dawson, V. L. Dawson, Understanding microRNAs in neurodegeneration. *Nat. Rev. Neurosci.* **10**, 837–841 (2009).
29. A. Riccio, Dynamic epigenetic regulation in neurons: Enzymes, stimuli and signaling pathways. *Nat. Neurosci.* **13**, 1330–1337 (2010).
30. G. Vitellius, S. Trabado, J. Bouligand, B. Delemer, M. Lombès, Pathophysiology of glucocorticoid signaling. *Ann. Endocrinol. (Paris)* **79**, 98–106 (2018).
31. G. Russell, S. Lightman, The human stress response. *Nat. Rev. Endocrinol.* **15**, 525–534 (2019).
32. S. Koyanagi *et al.*, Glucocorticoid regulation of ATP release from spinal astrocytes underlies diurnal exacerbation of neuropathic mechanical allodynia. *Nat. Commun.* **7**, 13102 (2016).
33. G. Blackburn-Munro, R. Blackburn-Munro, Pain in the brain: Are hormones to blame? *Trends Endocrinol. Metab.* **14**, 20–27 (2003).
34. G. Laumet *et al.*, G9a is essential for epigenetic silencing of K(+) channel genes in acute-to-chronic pain transition. *Nat. Neurosci.* **18**, 1746–1755 (2015).
35. A. Barski *et al.*, High-resolution profiling of histone methylations in the human genome. *Cell* **129**, 823–837 (2007).
36. B. Schuettengruber, D. Chourrout, M. Vervoort, B. Leblanc, G. Cavalli, Genome regulation by polycomb and trithorax proteins. *Cell* **128**, 735–745 (2007).
37. S. Gupta-Agarwal *et al.*, G9a/GLP histone lysine dimethyltransferase complex activity in the hippocampus and the entorhinal cortex is required for gene activation and silencing during memory consolidation. *J. Neurosci.* **32**, 5440–5453 (2012).
38. Z. Li *et al.*, The transcription factor C/EBPβ in the dorsal root ganglion contributes to peripheral nerve trauma-induced nociceptive hypersensitivity. *Sci. Signal.* **10**, eaam5345 (2017).
39. N. A. Datson *et al.*, Specific regulatory motifs predict glucocorticoid responsiveness of hippocampal gene expression. *Endocrinology* **152**, 3749–3757 (2011).
40. M. M. Jagodic *et al.*, Cell-specific alterations of T-type calcium current in painful diabetic neuropathy enhance excitability of sensory neurons. *J. Neurosci.* **27**, 3305–3316 (2007).
41. B. Coste, M. Crest, P. Delmas, Pharmacological dissection and distribution of NaN/Nav1.9, T-type Ca2+ currents, and mechanically activated cation currents in different populations of DRG neurons. *J. Gen. Physiol.* **129**, 57–77 (2007).
42. Q. Y. Liu *et al.*, Upregulation of $Ca_V3.2$ T-type calcium channels in adjacent intact L4 dorsal root ganglion neurons in neuropathic pain rats with L5 spinal nerve ligation. *Neurosci. Res.* **142**, 30–37 (2019).
43. S. F. Lin *et al.*, Colocalization of insulin-like growth factor-1 receptor and T type Cav3.2 channel in dorsal root ganglia in chronic inflammatory pain mouse model. *Neuroreport* **27**, 737–743 (2016).
44. M. Watanabe *et al.*, Expression and regulation of Cav3.2 T-type calcium channels during inflammatory hyperalgesia in mouse dorsal root ganglion neurons. *PLoS One* **10**, e0127572 (2015).
45. R. B. Messinger *et al.*, In vivo silencing of the Ca(V)3.2 T-type calcium channels in sensory neurons alleviates hyperalgesia in rats with streptozocin-induced diabetic neuropathy. *Pain* **145**, 184–195 (2009).
46. S. M. Todorovic, V. Jevtovic-Todorovic, Targeting of CaV3.2 T-type calcium channels in peripheral sensory neurons for the treatment of painful diabetic neuropathy. *Pflugers Arch.* **466**, 701–706 (2014).
47. M. M. Jagodic *et al.*, Upregulation of the T-type calcium current in small rat sensory neurons after chronic constrictive injury of the sciatic nerve. *J. Neurophysiol.* **99**, 3151–3156 (2008).
48. K. Okubo *et al.*, Inhibition of T-type calcium channels and hydrogen sulfide-forming enzyme reverses paclitaxel-evoked neuropathic hyperalgesia in rats. *Neuroscience* **188**, 148–156 (2011).
49. J. Yue, L. Liu, Z. Liu, B. Shu, Y. Zhang, Upregulation of T-type Ca2+ channels in primary sensory neurons in spinal nerve injury. *Spine* **38**, 463–470 (2013).
50. M. Montera *et al.*, Trigeminal neuropathic pain is alleviated by inhibition of $Ca_V3.3$ T-type calcium channels in mice. *Channels (Austin)* **15**, 31–37 (2021).
51. J. B. McCallum, W. M. Kwok, M. Mynlieff, Z. J. Bosnjak, Q. H. Hogan, Loss of T-type calcium current in sensory neurons of rats with neuropathic pain. *Anesthesiology* **98**, 209–216 (2003).
52. L. J. A. Kogelman *et al.*, Whole transcriptome expression of trigeminal ganglia compared to dorsal root ganglia in *Rattus norvegicus*. *Neuroscience* **350**, 169–179 (2017).
53. G. J. Bennett, Y. K. Xie, A peripheral mononeuropathy in rat that produces disorders of pain sensation like those seen in man. *Pain* **33**, 87–107 (1988).
54. Y. B. Martin, C. Avendaño, Effects of removal of dietary polyunsaturated fatty acids on plasma extravasation and mechanical allodynia in a trigeminal neuropathic pain model. *Mol. Pain* **5**, 8 (2009).
55. D. Christensen, M. Gautron, G. Guilbaud, V. Kayser, Combined systemic administration of the glycine/NMDA receptor antagonist, (+)-HA966 and morphine attenuates pain-related behaviour in a rat model of trigeminal neuropathic pain. *Pain* **83**, 433–440 (1999).
56. B. P. Vos, A. M. Strassman, R. J. Maciewicz, Behavioral evidence of trigeminal neuropathic pain following chronic constriction injury to the rat's infraorbital nerve. *J. Neurosci.* **14**, 2708–2723 (1994).
57. W. J. Dixon, Efficient analysis of experimental observations. *Annu. Rev. Pharmacol. Toxicol.* **20**, 441–462 (1980).
58. R. Qi *et al.*, Non-coding RNA profiling by high throughput sequencing. National Center for Biotechnology Information Gene Expression Omnibus. https://www.ncbi.nlm.nih.gov/geo/query/acc.cgi?acc=GSE192803. Deposited 30 December 2021.